Ukrainian Journal of Physical Optics
ISSUE 1
2025

OPTICAL EDGE DISLOCATION GENERATED WITH THE NEMATIC θ–CELL

O. KRUPYCH [1,2], T. DUDOK[1], I. SKAB[1], YU. NASTISHIN[3], Z. HRABCHAK[3], YE. RYZHOV[3], O. BULUY[4], P. ZELENOV[4], V. NAZARENKO[4,5], O. KUROCHKIN[4,5] AND R. VLOKH[1*]

[1] Vlokh Institute of Physical Optics, Ivan Franko National University of Lviv, 23 Dragomanov Str., Lviv 79005, Ukraine
[2] Department of Optoelectronics and Information Technologies, Ivan Franko National University of Lviv, 107 Tarnavskogo Str., Lviv 79017, Ukraine
[3] Hetman Petro Sahaidachnyi National Army Academy, 32 Heroes of Maidan Str., Lviv 79012, Ukraine
[4] Institute of Physics, National Academy of Sciences of Ukraine, 46 Nauky Ave., Kyiv 03028, Ukraine
[5] Institute of Physical Chemistry, Polish Academy of Sciences, Kasprzaka 44/52, 01-224 Warsaw, Poland
*Corresponding author: vlokh@ifo.lviv.ua

Received: 16.01.2025

Abstract. An optical edge dislocation is visualized as a shift of interference fringes in the Mach-Zehnder interferograms of the wavefront of a laser beam behind a nematic θ-cell with the circular and linear planar alignments of the nematic director on the opposite substrates. Using the approach of differential Jones matrices we establish that the half-period shift of the interference fringes addresses the π optical phase shift in the domains with the opposite handedness of the director twist on both sides of the nematic disclination separating these domains.

Keywords: optical edge dislocation, optical vortex, nematic θ-cell, nematic q-plate, enantiomorphic domains, optical phase shift
UDC: 535.4, 535.5
DOI: 10.3116/16091833/Ukr.J.Phys.Opt.2025.01064

1. Introduction

The singular beams bearing optical vortices have become an intriguing subject of study in recent decades. The interest of researchers in optical vortices is caused by their application in novel branches of optical technologies such as optical trapping and manipulation of the microparticles [1], quantum cryptography [2], quantum teleportation [3], light focusing below the diffraction limit [4], multiplexing and demultiplexing in the transmission of information [5], quantum computing [6], etc. These applications require developing simple and inexpensive methods of generating optical vortices. At least, the following known methods and tools for generating the beams bearing orbital angular momentum (OAM) can be listed at present: diffraction method on the computer-synthesized forked holograms [7], spiral phase plates [8], q-plates [9], crystal optical method under application of non-uniform fields [10-12], nanoscale metasurfaces [13], spatial light modulators [14], etc. Among them, probably the easiest in fabrication and most widely used are q-plates. A q-plate can be fabricated as a nematic liquid crystal (LC) cell doped with an azo-dye using the photo-alignment technique while rotating both the cell and linear polarizer [15]. A simple and

cheap technique for fabricating the LC cells with surface alignment singularities proposed in [16] does not require such expensive/laborious techniques as photo-lithography or polymer photo-alignment. As reported in [17], a *q*-plate can be produced using a nematic LC cell assembled of two circularly rubbed substrates.

A common drawback of available *q*-plates is that their design concepts do not imply switching the optical vortex charge. In contrast, our recent work [18] demonstrates that the topological charge of an optical vortex can be reversibly switched from $|l| = 1$ to $|l| = 2$ and back by an applied voltage to the so-called nematic θ–cell as a *q*–plate, while still employing techno–logically simple surface rubbing alignment to form nematic defects. The θ-cell [19-22] is called in [18] a CL cell for the reason that it is assembled from rubbed polymer-covered substrates that provide circular (C) and linear (L) planar alignment of the nematic director. As shown in [18], though for a nematic point defect of the topological strength s=+1 formed due to the circular rubbing of the substrate one expects the generation of the optical vortex of the topological charge $|l| = 2$, because of the optical activity due to the nematic director twist produced by the difference in the alignment at the opposite substrate surfaces, the vortex charge is reduced to $|l| = 1$. Application of the voltage between the substrates reorients the nematic director in the bulk towards the cell normal direction, consequently eliminating the director twist, vanishing the optical activity, and thereby switching the vortex charge from $|l| = 1$ to $|l| = 2$ [18].

However, this is not the end of the story. Since by its symmetry the nematic is achiral, both signs of the director twist are energetically equivalent and allowed, the nematic sample in the θ–cell splits into two domains with the opposite directions of the director twist. In nematics, an expected domain wall reduces to a line disclination, which on the polarization optical microscopy (POM) texture is observed parallel to the rubbing direction of the opposite substrate (Fig. 1) along the rubbing circles diameter. Our Mach-Zehnder interferograms shown in Figs. 1b, 2a,b indicate that the disclination line visible in Fig. 1b forms an edge dislocation in the laser beam behind the θ–cell. In the terminology, introduced by Nye and Berry [23] (see also [24,25]) wavefront dislocations in a laser beam can be of one of the three main types: a point edge dislocation (localized interference fringe in terminology [23]), screw dislocation and infinitely extended edge dislocation visualized as a nonlocalized interference fringe [23]. The interference pattern observed for the θ–cell in Figs. 1b, 2a,b visualizes the very such an optical edge dislocation.

The aim of this paper is to establish the origin of the optical edge dislocation observed for the θ–cell as a nonlocalized interference fringes in the Mach-Zehnder interferograms. We show that the half-period shift in the interference patter in Figs. 1b, 2a,b, *per se* revealing the optical edge dislocation, results from the optical phase difference of π between the waves propagating in the domains with the opposite director twist (enantiomorphic domains).

2. Experimental methods

In our experiments the cells of the thicknesses d=5 and ~20 μm were filled with commercial nematics MLC6609 and 6CHBT; both from Merck with the birefringence values 0.077 [26]) and 0.15 [27]).The nematic 6CHBT shows positive dielectric anisotropy while for MLC6609 it is negative.

The polarimetric images have been obtained using a collimated beam and the LC cells inserted between crossed linear polarizers. To visualize the optical singularities of light

beams transmitted through the studied LC cells, we used the interference patterns formed by a Mach–Zehnder interferometer in the manner, described in our recent paper (Ref. [28]). A studied sample was placed into the test arm of the interferometer between the crossed circular polarizers in order to achieve a pure vortex mode. The circular polarizers were assembled of linear polarizers aligned parallel to each other and quarter-wave plates with their optic axes at +45° and −45° with respect to the polarizers axes. In another interferometer arm, the reference arm, a divergent light beam is formed. The wide collimated beam of ~ 15 mm aperture was transmitted through the sample. The spherical wavefront of the wave propagated in the reference arm was formed using the positive lens with the focal length of 1 m. Resulting interference patterns for the vortex beams were recorded with a CCD camera.

The AC voltage with a root mean square values in the range of 0-10 V and frequency f=1 kHz were applied to the inner sides of substrates covered with a conducting layer of indium tin oxide for the cells filled with 6CHBT. Because of the negative dielectric anisotropy, there is no reason to apply such a transverse voltage to the MLC6609 cells. To produce the planar (parallel to the substrate surface) director alignment the conducted layers were covered with the polyimide layer PI2555 (from Nissan Chemicals). To produce the C and unidirectional L alignments of the director the polymer layers on the substrates were respectively circularly and unidirectionally mechanically rubbed.

3. Results and discussion

To establish the origin of the optical edge dislocation visualized in Figs. 1b, 2a,b one has to derive the analytical expression for the electric field of the light waves passing through the enantiomorphic domains separated by line disclination seen in Fig. 1a. The form of the light wave behind a twisted nematic (also called the cholesteric, preferentially for submicron pitches) can be found in the approach of differential Jones matrices for a cholesteric developed in [29,30]. In the framework of Jones calculus, the light wave exiting the analyzer in the test arm of the interferometer can be found as follows:

$$\vec{E}_{\pm} = AQ_{-\pi/4}J_M(\pm qz)Q_{+\pi/4}\vec{E}_0\,, \tag{1}$$

where $\vec{E}_{\pm}$ is the electric field vector of light wave, outgoing different domains in the vicinity of disclination line and exiting the circular analyzer, $\vec{E}_0 = P\vec{E}_{00}$ is the Jones vector of the normally incident linearly polarized light obtained from a light wave $\vec{E}_{00}$, exiting the polarizer P, $Q_{\pm\pi/4}$ are the quarter-wave plates with their axis rotated respectively by $\pm\pi/4$ with respect to the polarizer such that $Q_{+\pi/4}Q_{-\pi/4} = I$, where I is the unity matrix; $J_M(\pm qz)$ is the Jones matrix of a nematic twisted with the wave number $q = \pm 2\pi/p$ (± stands for the twists of opposite handedness in different domains) in the Mauguine (subscript M) regime; z is the running coordinate along the normal to the cell such that for a normally incident light beam, z=0 at the entrance surface of the nematic and z=d at its exit. The analyzer A=P is a polarizer parallel to that of the entrance polarizer P. In the Mauguine regime, the integral matrix for a twisted nematic is of the form (see Eq. 61 in [29]):

$$J_M(\pm qz) = R(\pm qz)\exp\left[\left(N^0 - (\pm q)R(\pi/2)\right)z\right], \tag{2}$$

with

$$N^0 = -\frac{2\pi}{\lambda} i \begin{pmatrix} n_\perp & 0 \\ 0 & n_\parallel \end{pmatrix}, \tag{3}$$

being the differential Jones matrix of a nematic, in which $n_\perp$ and $n_\parallel$ are the ordinary and extraordinary refractive indices measured for the light polarization set, respectively perpendicular ($\perp$) and parallel ($\parallel$) to the nematic director and

$$R(\pm qz) = \begin{pmatrix} \cos(\pm qz) & -\sin(\pm qz) \\ \sin(\pm qz) & \cos(\pm qz) \end{pmatrix}; \quad R(\pi/2) = \begin{pmatrix} 0 & -1 \\ 1 & 0 \end{pmatrix}, \tag{4}$$

being the rotation Jones matrices. At $q\lambda/2\pi = \lambda/p \ll 1$, the Mauguine regime reduces to the so-called adiabatic regime [29].

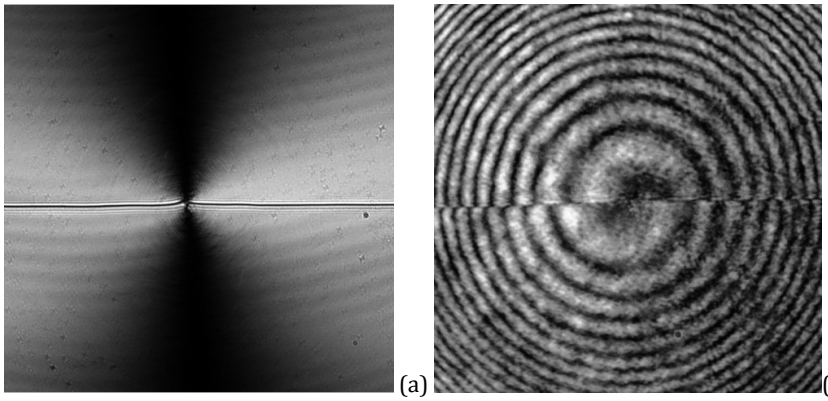

(a) (b)

Fig. 1. The MLC6609 θ-cell (d=20 μm,) viewed between crossed linear polarizers (a) and its Mach-Zehnder interferogram (b) at zero applied voltage.

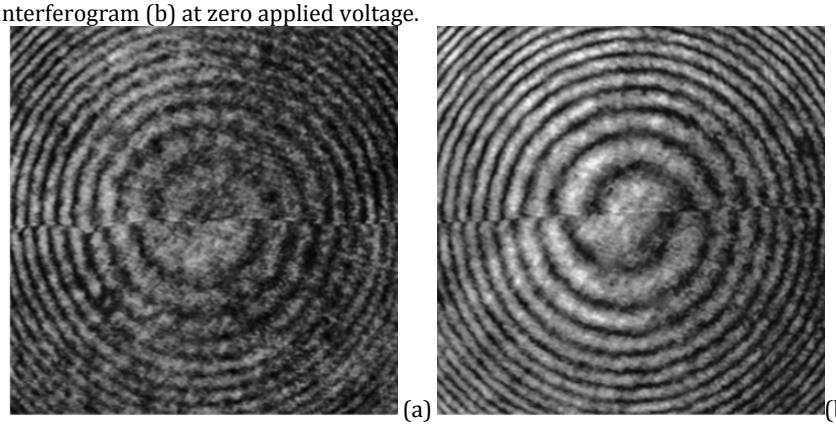

(a) (b)

Fig. 2. Mach-Zehnder interference patterns with the dislocation for 5 μm (a) 6CHBT cell and (b) MLC6609 cells of 5 μm thickness at zero applied voltage.

The disclination line separating the enantiomorphic domains is shown in Fig. 1a for the 20 μm MLC6609 cell. Quite similar polarimetric textures are observed for the 5 μm MLC6609 cell and 6CHBT cells of both (5 and 20 μm) thickness values. For this reason these POM textures are not shown here. The single extinction brush (instead of two brushes) manifests the rotation of the polarization plane in the horizontal plane by $\pm\pi/2$ angle on the different sides of the disclination line. It is seen in Figs. 1b and 2, that the interference fringes are mutually shifted by half the period of the interference pattern for the domains separated by the horizontal defect line.

For the rotation of the director by $\pi/2$ the pitch of the director twist $p=4d$ and, thus, for the θ-cells of $d\approx 5$μm and $d\approx 20$μm at $\lambda=0.6328\,\mu$m for the direction along the disclination line one has $\lambda/p\approx 0.03$ and 0.008, respectively. Therefore, for the θ-cells of both thicknesses one has $\lambda/p\ll 1$ and thus $J_M(\pm qz)$ reduces to:

$$J_a(\pm qz)=R(\pm qz)e^{N^0 z}, \tag{5}$$

where the subscript *a* denotes the adiabatic regime.
The substitution of

$$\vec{E}_0=\begin{bmatrix}1\\0\end{bmatrix},\ P=\begin{bmatrix}1&0\\0&0\end{bmatrix},\ Q_{\pm\pi/4}=\frac{1}{\sqrt{2}}\begin{bmatrix}1&\mp i\\ \mp i&1\end{bmatrix}, \tag{6}$$

in Eq. (1) gives:

$$\vec{E}_{\pm}=\exp\left\{-i\left(\frac{2\pi}{\lambda}\bar{n}\mp q\right)z\right\}\cos\left(\pi\frac{\Delta nz}{\lambda}\right). \tag{7}$$

At the exit of the twisted nematic one has *z=d* with $\mp qd=\mp\pi/2$ on the different sides of the disclination line and thus

$$\vec{E}_{\pm}\big|_{z=d}=\exp\left\{-i\frac{2\pi}{\lambda}\left(\bar{n}d\mp\frac{\lambda}{4}\right)\right\}\cos\left(\pi\frac{\Delta nd}{\lambda}\right). \tag{8}$$

Eq. (8) shows that the optical passes of the light waves $\vec{E}_+$ and $\vec{E}_-$ exiting the nematic domains with the opposite twist handedness respectively are $\bar{n}d-\lambda/4$ and $\bar{n}d+\lambda/4$, thus differing by $\lambda/2$, which is equivalent to the phase difference of π and thereby inevitably forming a dislocation at the contact of their wave fronts when interfering with the light wave of the reference arm, except at the condition $\Delta nd=(2m+1)\lambda/2$, for which one has $\cos[\pi(2m+1)/2]=0$ with $m=0,1,2,\ldots$ being an integer number. We believe that Fig. 3(a) in which the dislocation is hardly observed, corresponds to very such a case when in Eq. (8), $\Delta nd=(2m+1)\lambda/2$. The value of the path difference $D=\Delta nd$ of the eigenwaves can be varied by the application of the voltage to the cell. Under the applied voltage, the director of a nematic with the positive dielectric anisotropy $\Delta\varepsilon>0$ tends to realign along the field direction. As a result, the path difference $D=\Delta nd$ transforms into:

$$D_{eff}=\int_0^d \Delta n\sin^2\theta(z)dz, \tag{9}$$

where θ is the angle between the nematic director and the light propagation direction, which is along the cell normal. Therefore, one can expect that reducing D_{eff} with the applied voltage, one can escape the condition $D_{eff}=(2m+1)\lambda/2$.

The analysis of Fig. 3 shows that the disclination is poorly visible at zero applied voltage (Fig. 3a), but becomes better visible when the voltage increases above the threshold voltage (0.76 V) to 1.0V (Fig. 3b), and then on further voltage increase it is again hardly visible at 1.9 V (Fig. 3c), and then again is better visible at 2.1 V (Fig. 3d). Here, poor/better visibility of the disclination should be understood as poor/better contrast of the interferogram as well as the absence/presence of the shift of the interference patterns below and above the border between the domains of opposite handedness. Eq. (8) suggests that due to the periodicity of

the factor $\cos(\pi\Delta nd/\lambda)$, the brightness of the pattern resulting of interference of orthogonal linearly polarized eigenwaves depend on the phase difference $\Delta\Gamma = \pi\Delta nd/\lambda$. When the phase difference is equal to $\Delta\Gamma = (2m+1)\pi/2$ (m is the integer number), the expression in the right part of Eq. (8) is reduced to zero. Therefore, we are led to conclude that poor visibility of the disclination in the interferograms at zero applied voltage in the 20 μm CL filled with 6CHBT is rather an incidence (Fig. 3a), while the disclination is clearly visible in the 20 μm CL cell filled with MLC6609 (Fig. 1(b)) as well as in 5 μm CL cells with 6CHBT (Fig. 2(a)) and MLC6609 (Fig. 2(b)).

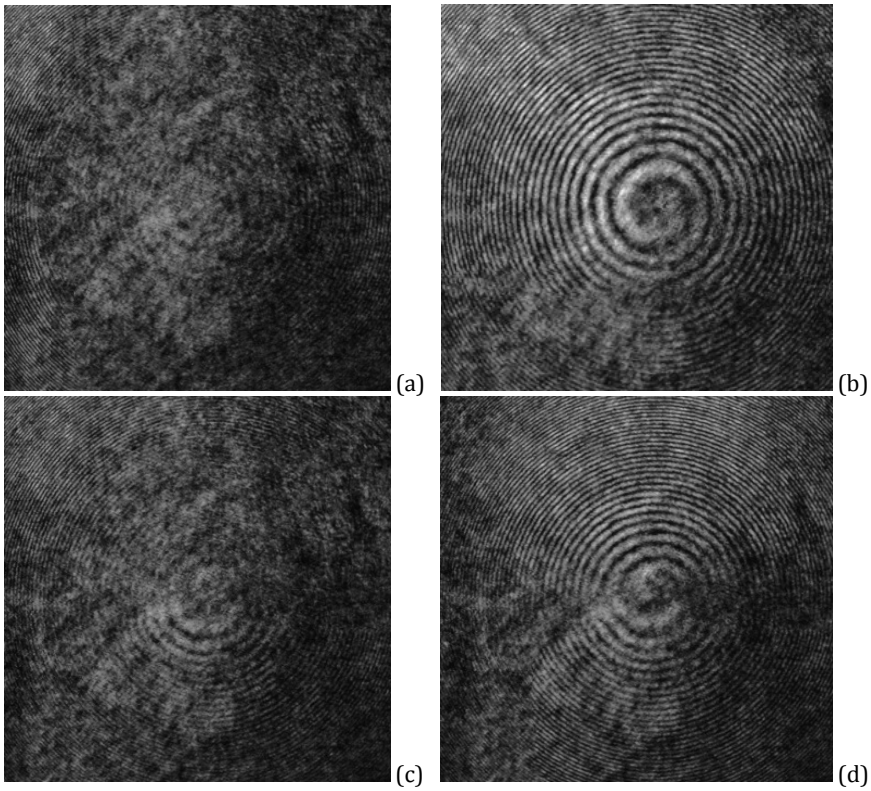

Fig. 3. Mach-Zehnder interferograms for the 20 μm cell filled with the nematic 6CHBT at (a) 0 V, (b) 1.0V, (c) 1.9 V and (d) 2.1 V.

Generally, the studied θ-cell can be considered as an optical medium, in which the linearly polarized light normally incident rotates by π/2 exiting the cell. In this case, mathematically, one can decompose the incident linearly polarized light into two waves with the opposite-handedness of circular polarization and the same amplitudes propagating through the sample with different velocities (see e.g. [31]). In this case, the angle of polarization plane rotation is determined as follows:

$$\varphi = \frac{1}{2}\Delta\Gamma_C = \frac{\pi d}{\lambda}c\left(\frac{1}{v_r} - \frac{1}{v_l}\right) \tag{10}$$

where v_r and v_l are the velocities of right-handed and left-handed waves, respectively, c is the speed of light in vacuum, and $\Delta\Gamma_C$ is the phase difference between these waves on the distance d. It is obvious from Eq. (10) that when the angle of polarization plane rotation is

equal to $\varphi = \pi/2$, the phase difference between left and right-handed circular waves is $\Delta\Gamma_c = \pi$. Therefore, if the circular incident wave is, e.g., left-handed in the domain with the right-handed twist structure, this wave is the fast wave, while in the left-handed domain, it is the slow wave. Thus, the interference of these waves with the reference wave is constructive in the first domain, while destructive in the second one. Such a generalized consideration can be a simple explanation for the half-period shift of interference fringes without going into details of light propagation within a twisted nematic.

4. Conclusion

In addition to an optical vortex, which is a screw dislocation in the wavefront of a laser beam behind a nematic θ-cell cell with the circular and linear planar alignment of the nematic director on the opposite substrates, an optical edge dislocation is generated and visualized as a shift of interference fringes in the in the Mach-Zehnder interferograms. While the optical vortex is formed when the laser beam passes through the nematic circular point defect, the optical edge dislocation appears in the place where the light hits the nematic disclination line, which separates the domains with the opposite handedness of the director twist. In the terminology introduced by Nye and Berry such an optical edge dislocation corresponds to a nonlocalized interference fringe on the interferogram. Using the Jones calculus approach we have established the origin of this optical edge dislocation. We prove that that the shift in the Mach-Zehnder interference fringes is due to the π phase shift, produced by the opposite handedness of the director twist in the domains separated by the nematic disclination.

Acknowledgement. Authors, affiliated in (1) acknowledge the Ministry of Education and Science of Ukraine for financial support of the present work (projects No. 0124U000979) and NASU (project No. 0123U100832). This work was supported by the Long-term program of support of the Ukrainian research teams at the PAS Polish Academy of Sciences carried out in collaboration with the U.S. National Academy of Sciences with the financial support of external partners via the agreement No. PAN.BFB.S.BWZ.356.022.2023; the NATO Science for Peace and Security Programme grant SPS G6030.

References

1. Grier, D. G. (2003). A revolution in optical manipulation. *Nature*, *424*(6950), 810-816.
2. Sit, A., Fickler, R., Alsaiari, F., Bouchard, F., Larocque, H., Gregg, P., Yan, L., Boyd, R.W., Ramachandran, S., & Karimi, E. (2018). Quantum cryptography with structured photons through a vortex fiber. *Optics Letters*, *43*(17), 4108-4111.
3. Boschi, D., Branca, S., De Martini, F., Hardy, L., & Popescu, S. (1998). Experimental realization of teleporting an unknown pure quantum state via dual classical and Einstein-Podolsky-Rosen channels. *Physical Review Letters*, *80*(6), 1121.
4. Quabis, S., Dorn, R., Eberler, M., Glöckl, O., & Leuchs, G. (2000). Focusing light to a tighter spot. *Optics Communications*, *179*(1-6), 1-7.
5. Krenn, M., Handsteiner, J., Fink, M., Fickler, R., Ursin, R., Malik, M., & Zeilinger, A. (2016). Twisted light transmission over 143 km. *Proceedings of the National Academy of Sciences*, *113*(48), 13648-13653.
6. DiVincenzo, D. P. (1995). Quantum computation. *Science*, *270*(5234), 255-261.
7. Bazhenov, V. Y., Vasnetsov, M. V., & Soskin, M. S. (1990). Laser beams with screw dislocations in their wavefronts. *JETP Lett*, *52*(8), 429-431.
8. Beijersbergen, M. W., Coerwinkel, R. P. C., Kristensen, M., & Woerdman, J. P. (1994). Helical-wavefront laser beams produced with a spiral phaseplate. *Optics Communications*, *112*(5-6), 321-327.
9. Marrucci, L., Manzo, C., & Paparo, D. (2006). Optical spin-to-orbital angular momentum conversion in inhomogeneous anisotropic media. *Physical Review Letters*, *96*(16), 163905.

10. Skab, I., Vasylkiv, Y., Savaryn, V., & Vlokh, R. (2011). Optical anisotropy induced by torsion stresses in $LiNbO_3$ crystals: appearance of an optical vortex. *JOSA A*, *28*(4), 633-640.
11. Skab, I., Vasylkiv, Y., Zapeka, B., Savaryn, V., & Vlokh, R. (2011). Appearance of singularities of optical fields under torsion of crystals containing threefold symmetry axes. *JOSA A*, *28*(7), 1331-1340.
12. Skab, I., Vasylkiv, Y., Smaga, I., & Vlokh, R. (2011). Spin-to-orbital momentum conversion via electro-optic Pockels effect in crystals. *Physical Review A*, *84*(4), 043815.
13. Devlin, R. C., Ambrosio, A., Rubin, N. A., Mueller, J. B., & Capasso, F. (2017). Arbitrary spin-to–orbital angular momentum conversion of light. *Science*, *358*(6365), 896-901.
14. Ostrovsky, A. S., Rickenstorff-Parrao, C., & Arrizón, V. (2013). Generation of the "perfect" optical vortex using a liquid-crystal spatial light modulator. *Optics Letters*, *38*(4), 534-536.
15. Huang, Y. H., Li, M. S., Ko, S. W., & Fuh, A. Y. G. (2013). Helical wavefront and beam shape modulated by advanced liquid crystal q-plate fabricated via photoalignment and analyzed by Michelson's interference. *Applied Optics*, *52*(26), 6557-6561.
16. Clark, N. A. (1985). Surface memory effects in liquid crystals: Influence of surface composition. *Physical Review Letters*, *55*(3), 292.
17. Marrucci, L., Manzo, C., & Paparo, D. (2006). Pancharatnam-Berry phase optical elements for wave front shaping in the visible domain: switchable helical mode generation. *Applied Physics Letters*, *88*(22).
18. Krupych, O., Dudok, T., Skab, I., Nastishin, Yu., Hrabchak, Z., Chernenko, A., Buluy, O., Zelenov, P., Nazarenko, V., Kurochkin, o., Vlokh, R. (2025). Electric field controlled switching of an optical vortex charge with a liquid crystal cell. *Optics Communication*. *579*, 131593.
19. Stalder, M., & Schadt, M. (1996). Linearly polarized light with axial symmetry generated by liquid-crystal polarization converters. *Optics Letters*, *21*(23), 1948-1950.
20. Suh, S. W., Joseph, K., Cohen, G., Patel, J. S., & Lee, S. D. (1997). Precise determination of the cholesteric pitch of a chiral liquid crystal in a circularly aligned configuration. *Applied Physics Letters*, *70*(19), 2547-2549.
21. Vasnetsov, M. V., Kasyanyuk, D. S., Terenetskaya, I. P., Kapinos, P. S., & Slyusar, V. V. (2013). Disclination line in θ-cell as an indicator of liquid crystal chirality. *Molecular Crystals and Liquid Crystals*, *575*(1), 57-63.
22. Kurochkin, O., Nazarenko, K., Tereshchenko, O., Golub, P., & Nazarenko, V. (2023). The helical twisting power of chiral dopants in lyotropic chromonic liquid crystals. *Liquid Crystals*, *50*(1), 110-120.
23. Nye, J. F., & Berry, M. V. (1974). Dislocations in wave trains. *Proceedings of the Royal Society of London. A. Mathematical and Physical Sciences*, *336*(1605), 165-190.
24. Soskin, M. S., Vasnetsov, M. V., & Basistiy, I. V. (1995, November). Optical wavefront dislocations. In *International Conference on Holography and Correlation Optics* (Vol. 2647, pp. 57-62). SPIE.
25. Basistiy, I. V., Soskin, M. S., & Vasnetsov, M. V. (1995). Optical wavefront dislocations and their properties. *Optics Communications*, *119*(5-6), 604-612.
26. Li, F., Buchnev, O., Cheon, C. I., Glushchenko, A., Reshetnyak, V., Reznikov, Y., Sluckin, T.J. & West, J. L. (2006). Orientational coupling amplification in ferroelectric nematic colloids. *Physical Review Letters*, *97*(14), 147801.
27. Domański, A., Budaszewski, D., Sierakowski, M., & Woliński, T. (2006). Depolarization of partially coherent light in liquid crystals. *Opto-Electronics Review*, *14*(4), 305-310.
28. Dudok, T., Skab, I., Mys, O., Krupych, O., Nastishin, Yu. A., Kurochkin, O., Nazarenko, V., Ryzhov, Ye., Chernenko, A. D., & Vlokh R. (2023). Optical vector vortices generated with circularly planar and circularly hybrid nematic cells. *Ukrainian Journal of Physical Optics*, *24*(1), 22-45.
29. Nastyshyn, S. Y., Bolesta, I. M., Tsybulia, S. A., Lychkovskyy, E., Yakovlev, M. Y., Ryzhov, Y., Vankevych, P. I. & Nastishin, Y. A. (2018). Differential and integral Jones matrices for a cholesteric. *Physical Review A*, *97*(5), 053804.
30. Nastyshyn, S. Y., Bolesta, I. M., Tsybulia, S. A., Lychkovskyy, E., Fedorovych, Z. Y., Khaustov, D. Y., Ryzhov, P. I. Vankevych, & Nastishin, Y. A. (2019). Optical spatial dispersion in terms of Jones calculus. *Physical Review A*, *100*(1), 013806.
31. Ditchburn, R.W. (1953). *Light*. Blackie & Son Limited, Hardcover.

O. Krupych, T. Dudok, I. Skab, Yu. Nastishin, Z. Hrabchak, Ye. Ryzhov, O. Buluy, P. Zelenov,V. Nazarenko, O. Kurochkin and R. Vlokh. (2025). Optical Edge Dislocation Generated with the Nematic θ – Cell**.** *Ukrainian Journal of Physical Optics*, *26*(1), 01064 – 01072.
doi: 10.3116/16091833/Ukr.J.Phys.Opt.2025.01064.

Анотація. *На основі зміщення інтерференційних смуг на інтерферограмах Маха-Цендера нами виявлена крайова дислокація оптичного хвильового фронту лазерного пучка, який поширюється через нематичну θ–комірку з круговим і лінійним планарним розташуванням нематичного директора на протилежних підкладках. Використовуючи підхід диференціальних матриць Джонса, встановлено, що півперіодний зсув інтерференційних смуг відповідає зсуву фаз рівному π в областях із протилежним напрямком повороту директора, тобто по різні боки від нематичної дисклінації, що розділяє ці області.*

Ключові слова: *крайова дислокація оптичного хвильового фронту, оптичний вихор, нематична θ–комірка, нематична q-пластинка, енантіоморфні домени, зсув фаз*